THE IUE DN159 DMU ANOMALY

I. Skillen

INSA/ESA-IUE Observatory, Apartado 50727, 28080 Madrid, Spain

Abstract

An objective method for the identification of IUE images affected by the DN159 DMU anomaly is described. It is shown from the perspective of its effect on science data that the onset of the anomaly most probably occurred during the first 23 days of $October, 1994$. In total, 1895 images influenced at the 3σ level are identified, and the degree to which they are corrupted is estimated.

Key words: IUE; DN159 Anomaly.

1 INTRODUCTION

An anomalous behaviour of the analogue-to-digital(A/D) converter of the Data Multiplexer Unit (DMU) on-board IUE was first noted on $24^{th} October, 1994$, when reaction wheel tach data points were seen sporadically to take on an erroneous value of Data Number (DN) 159. Subsequently, in $January, 1995$ science data were observed to be similarly affected; an image histogram showed a significant excess of pixels having DN159. This coincided with high DMU and On-Board Computer (OBC) temperatures of $55.8^o C$ and $25.6^o C$ respectively. Operational procedures were put in place to contain this behaviour, primarily by temperature management of the spacecraft and exposure-time adjustments. Nonetheless, DN159 corruption continued to affect engineering and science data on occasions until the end of orbital operations (see Peréz-Calpena & Pepoy, 1997).

Studies showed that the nature of the anomaly was such that raw data numbers in the range DN(160 − 191) were corrupted to a value of DN159. This was understood in terms of an erroneous decision at a particular stage in the successive approximation operation of the A/D converter. To illustrate this behaviour, Figure 1 shows the histogram of an exceptionally highly corrupted UV-FLOOD image (a well-exposed non-dispersed image of a calibration UV lamp). Note the depletion of pixels in the range DN(160 − 191), and the large excess at DN159. The distribution of pixels with DN values above 191 and below 159 appears to be unaffected. (A more representative example of a corrupt science image histogram is shown in Figure 5).

The aim of this study is to identify those science images affected by the DN159 anomaly, enabling them to be treated appropriately in the offline processing.
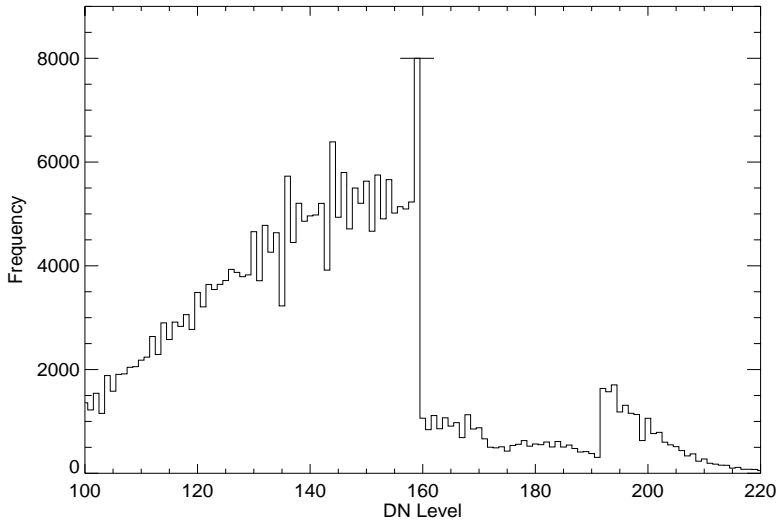
Figure 1: *Histogram of an excessively corrupted image showing the effect of the DN159 anomaly on pixels in the range DN(159 − 191). The frequency in bin 159 extends to 97872; it is truncated for clarity.*

2 RAW IMAGE ANALYSIS

2.1 Test Statistic

The *science image* was defined as the region of the raw image enclosed by the circle $(x - 384) = 344cos(\vartheta)$; $(y - 384) = 344sin(\vartheta)$, where $0 \leq \vartheta < 2\pi$. This was chosen to exclude the bright rim of the SWP camera, but to include the maximum extent of low- and high-resolution images. The same definition of the science image was applied to the LWP camera, although it does not exhibit a bright rim.

To identify an image as being affected by the DN159 anomaly, it is necessary to develop a test which discriminates between affected and unaffected images in an objective manner. A suitable test statistic is $\mathcal{E} = (O_{159} - F_{159})/\sigma_{159}$, where O_{159} is the actual number of pixels with DN159, F_{159} is related to the expected number having DN159, and σ_{159} is a measure of the histogram bin-to-bin scatter in the immediate neighbourhood of bin 159. Although $\mathcal{E}$ is expected to be approximately normally distributed, it is preferable to determine its distribution empirically by reference to images unaffected by the DMU anomaly. The test for DN159 corruption is then a test of the null hypothesis, at the 3σ level of significance, that the value of $\mathcal{E}$ for the image being tested is consistent with the general population of IUE images before the onset of the DMU anomaly. Rejection of the null hypothesis implies the image is considered to be affected by DN159 corruption.

2.2 Persistent Histogram Pattern

A feature of IUE image histograms, apparently present from the start of the project, complicates the determination of the distribution of the test statistic. This feature is a *persistent histogram pattern*, which occurs in several parts of the image histogram, one of which is bin 159. It is manifested there by the frequency in bin 159 persistently being less than,

2
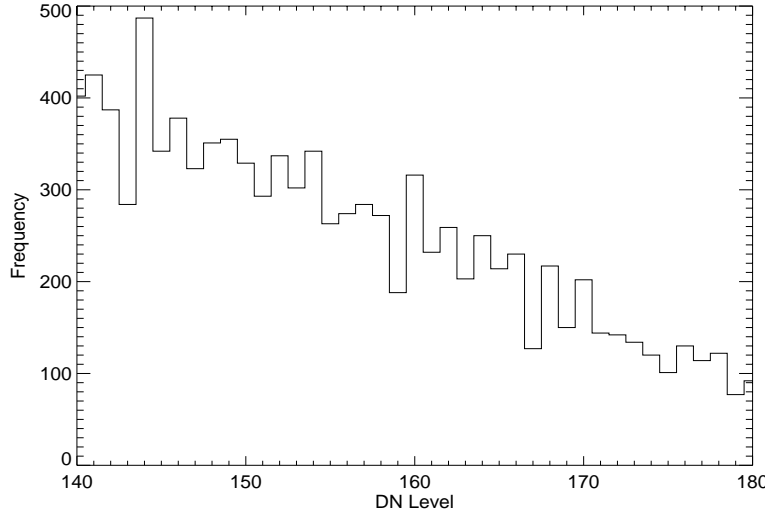
Figure 2: *Illustration of the persistent histogram pattern for $DN(143, 144)$ and $DN(159, 160)$.*

and the frequency in bin 160 being greater than, the frequencies in neighbouring bins (Figure 2). Furthermore, the degree of this effect scales with histogram frequency, F_{159}; for example, the histogram of a high resolution image will have a correspondingly greater diminution of pixels with DN159 (expressed in terms of σ_{159}) than will the histogram of a low resolution image. The effect of this is that we cannot consider a single distribution function of $\mathcal{E}$; instead we must consider the distribution functions $\mathcal{E}(F_{159})$, determined as a function of F_{159} (Figure 3). Therefore, any level of significance of $\mathcal{E}$ is a *contour* when plotted against F_{159}.
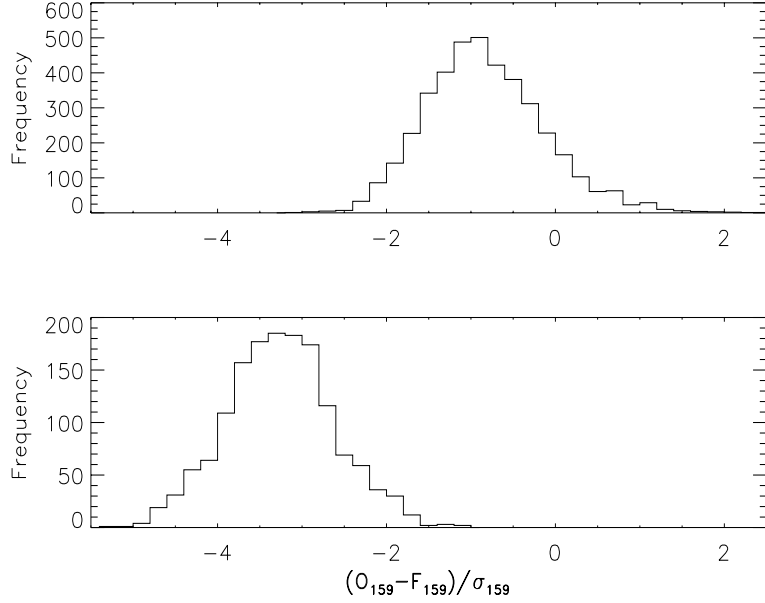
Figure 3: *Distributions of $\mathcal{E}$ for two bins of F_{159}, $5 \leq F_{159} < 6$ (top) and $300 \leq F_{159} < 500$ (bottom). The asymmetry in the top plot reflects small-number statistics in the image histograms.*

3

It is emphasised that this persistent histogram pattern is distinct from the DMU anomaly, and affects images over the lifetime of IUE. It most probably reflects a small bias in the A/D conversion process, and although its effect on any given image *pixel* is small, its effect on an image *histogram* is not.

2.3 Test Statistic Distribution

Approximately 30000 SWP and 20000 LWP raw images, mostly taken at Vilspa, and spanning the period 1978 to mid-$March$, 1993, were available on optical disks at the time this analysis was performed. These images formed the dataset used to derive the empirical distribution of $\mathcal{E}$, and its dependence on F_{159}. A further 3500 SWP and 3000 LWP Vilspa images from the period mid-$March$, 1993 to $23^{rd}October, 1994$ were retained as a control group (Section 4).

Segmented linear fits to the histogram of each science image in the bin intervals $(148-158)$ and $(161-170)$ were made, and F_{159} obtained from $F_{159}=(F1+F2)/2$, where $F1$ and $F2$ are extrapolations of the linear segments to bin 159. Similarly, σ_{159} was quantified by the standard deviation of the histogram bins about the segmented linear fits. Cases for which $|F1-F2|$ exceeds σ_{159} were flagged and examined visually to determine the best F_{159}. $\mathcal{E}$ $=(O_{159}-F_{159})/\sigma_{159}$ was then stored in bins delimited by: $0 \leq F_{159} < 1$, $1 \leq F_{159} < 2$, $2 \leq F_{159} < 3$,...,$10 \leq F_{159} < 12$,...,$20 \leq F_{159} < 25$, $25 \leq F_{159} < 50$,...,$100 \leq F_{159} < 150$..., and thus the dependence of $\mathcal{E}$ on F_{159} was quantified. Separate distributions were determined for the SWP and LWP cameras.

3 SIGNIFICANCE CONTOURS AND CONFIDENCE - INTERVALS OF $\mathcal{E}$

3.1 Empirical Determination

The modal value m, of each distribution $\mathcal{E}(F_{159})$ defines the contour of the most probable value of $\mathcal{E}(F_{159})$. Similarly, the limits enclosing 68% of each $\mathcal{E}(F_{159})$ about its mode, (θ_1, θ_2), correspond to the usual $\pm 1\sigma$ confidence interval for a normal distribution, and $\theta_1(F_{159})$ and $\theta_2(F_{159})$ therefore define the confidence interval of the most probable contour of $\mathcal{E}(F_{159})$. This interval becomes asymmetric for F_{159} less than ~ 15 due to the effect of small-number statistics in the image histograms.

The DN159 anomaly causes a *positive* deviation of the test statistic $\mathcal{E}$, and therefore a one-tailed significance test is appropriate. The 3σ significance contour cannot be derived empirically from $\mathcal{E}(F_{159})$ since there are insufficient images in each F_{159} bin (typically $500-1200$). Instead, a hybrid approach was adopted; the one-tailed 95% significance contour $\alpha_{95}(F_{159})$ *was* derived empirically, and the 3σ contour obtained from it by modelling the remaining extent of each tail of $\mathcal{E}(F_{159})$ by a normal distribution, that is, by extending the 95% significance contour by $1.355\theta_1(F_{159})$.

Mean contours were adopted for $\theta_1(F_{159})$ and $\theta_2(F_{159})$ and applied to each camera, since the differences between the contours derived individually for the two cameras are negligible.
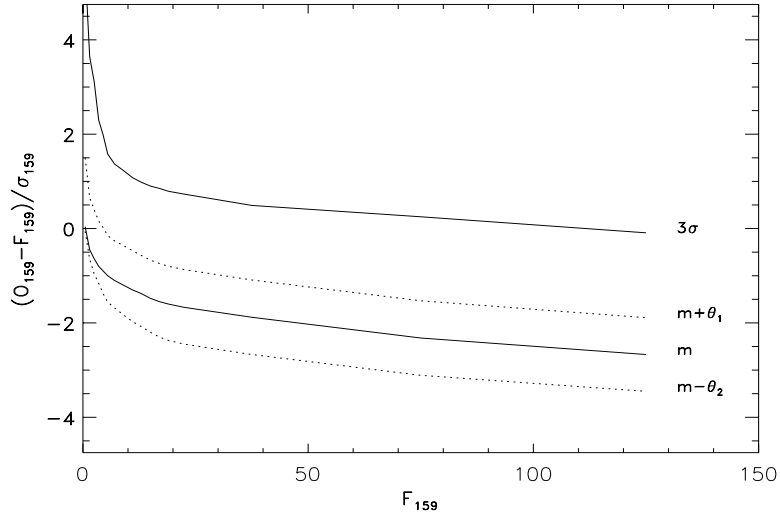
Figure 4: *Cubic spline representations of the 3σ, m and $m_{-\theta2}^{+\theta1}$ contours of $\mathcal{E}(F_{159})$ for the SWP camera.*

This is not the case for the $m(F_{159})$ and $3\sigma(F_{159})$ contours, where the differences are such that the two cameras must be treated independently. The results for the SWP and LWP cameras are summarised in Table 1, and the m, $m_{-\theta2}^{+\theta1}$ and 3σ contours are illustrated for the SWP camera in Figure 4.

3.2 Accuracy Of Significance Levels

The tolerances on the 95% and 3σ contours are approximated by the mean error of each $\mathcal{E}$ distribution used in their formation. In testing a sample of N images spanning the range of F_{159}, the uncertainty in the fraction exceeding a contour, $\alpha\%$, due to the sample itself is estimated as $\sqrt{(1 - \alpha/100)N}/N$, and the *total* uncertainty in the fraction exceeding α obtained by adding both uncertainties quadratically. For the sample sizes considered here, $\sim (3000 - 4000)$ images, we expect therefore $5\% \pm 0.75\%$ and $0.135\% \pm 0.06\%$ to exceed the 95% and 3σ contours respectively. Of the SWP and LWP images used to define the distribution of $\mathcal{E}$, 0.21% and 0.18% respectively exceed the corresponding 3σ contours, and it is concluded that both the SWP and LWP 3σ contours have been determined satisfactorily.

3.3 Test For DN159 Corruption

The objective test of an image, i, for DN159 corruption can now be stated. The values of $^{i}F_{159}$ and $^{i}\sigma_{159}$ are determined for the image by making segmented linear fits to its histogram, and the corresponding value of $^{i}\mathcal{E}$ computed. Cubic spline interpolation of the 3σ significance contour yields the 3σ value $^{i}\mathcal{E}_{3\sigma}$ against which this image is tested. If $^{i}\mathcal{E} > {}^{i}\mathcal{E}_{3\sigma}$, the null hypothesis of consistency with the general population of IUE images is rejected at the 3σ level, and the image is flagged as corrupt. In this case, cubic spline interpolations in the most probable and confidence interval contours yield the corresponding estimates of the most probable value of $\mathcal{E}$ and its uncertainty for this image, namely $^{i}m_{-i\theta2}^{+i\theta1}$. The most probable number of corrupt DN159 pixels in the image, C_{159}, is then obtained from $(^{i}\mathcal{E}$ -

5

Table 1: *Empirically derived contours of $\mathcal{E}(F_{159})$. The corresponding 3σ contours are* $3\sigma = \alpha_{95} + 1.355\theta_1$

	SWP Camera		LWP Camera			
F_{159}	α_{95}	m	α_{95}	m	θ_1	θ_2
0.5	$+3.55$	$+0.04$	$+3.08$	0.00	$+1.46$	$+0.10$
1.5	$+2.05$	-0.45	$+1.26$	-0.32	$+1.10$	$+0.20$
2.5	$+1.70$	-0.78	$+0.93$	-0.75	$+1.04$	$+0.32$
3.5	$+1.00$	-0.85	$+0.79$	-0.85	$+0.96$	$+0.36$
4.5	$+0.73$	-0.92	$+0.67$	-0.90	$+0.92$	$+0.48$
5.5	$+0.41$	-1.00	$+0.47$	-1.00	$+0.85$	$+0.56$
7.0	$+0.23$	-1.10	$+0.32$	-1.12	$+0.84$	$+0.58$
9.0	$+0.09$	-1.25	$+0.18$	-1.21	$+0.84$	$+0.63$
11.0	$+0.02$	-1.38	$+0.15$	-1.35	$+0.83$	$+0.65$
13.0	-0.06	-1.42	$+0.10$	-1.44	$+0.82$	$+0.68$
15.0	-0.15	-1.48	$+0.08$	-1.49	$+0.81$	$+0.72$
17.0	-0.25	-1.55	$+0.03$	-1.55	$+0.81$	$+0.75$
19.0	-0.29	-1.64	-0.02	-1.59	$+0.80$	$+0.77$
22.5	-0.35	-1.70	-0.10	-1.65	$+0.80$	$+0.78$
37.5	-0.58	-1.88	-0.36	-1.87	$+0.79$	$+0.79$
75.0	-0.82	-2.32	-1.10	-2.37	$+0.79$	$+0.79$
125.0	-1.15	-2.67	-1.40	-2.65	$+0.78$	$+0.78$
175.0	-1.50	-2.84	-1.62	-2.79	$+0.76$	$+0.76$
250.0	-1.78	-3.00	-1.81	-2.91	$+0.75$	$+0.75$
400.0	-2.09	-3.23	-2.16	-3.05	$+0.72$	$+0.72$
≥ 500.0	-2.10	-3.25	-2.16	-3.08	$+0.72$	$+0.72$

$^{i}m)_{+^{i}\theta2}^{-^{i}\theta1}$. This is illustrated in Figure 5 for image SWP56177, which is classified as corrupt. This image has $O_{159} = 309$ pixels, and the most probable number of corrupt pixels is $C_{159} = 168 \pm 14$. Note that due to the persistent histogram pattern, $F_{159} > 3\sigma$.

4   ONSET OF THE ANOMALY

The control group of 3500 SWP and 3000 LWP Vilspa images was tested against the 95% significance contours to determine the onset of the anomaly from the perspective of its effect on science data. The 95% contours were selected for this purpose because of the relatively small numbers of SWP and LWP images in the control group. For the LWP group, 4.8%±0.75% exceeded the 95% significance contour, which is consistent with expectations. However, for the SWP group, 9.5% ± 0.75% exceeded the 95% significance contour. The excess above 5% is $\sim$ 6 times greater than the uncertainty computed in Section 3.2.
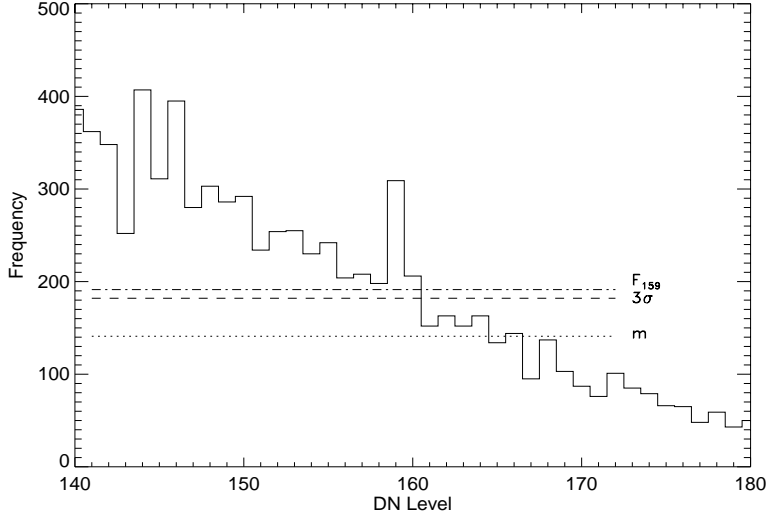
Figure 5: *Histogram of a corrupt image showing F_{159} as determined from segmented linear fits, and the most probable, m, and 3σ estimates of the number of non-corrupt DN159 pixels in the image.*

To investigate this further, analyses were made of samples of the SWP control group, each sample being defined by truncating the control group at the end of *December*, 1993, *January*, 1994,...,*September*, 1994. For each of the 10 samples thus formed, $5\% - 6.2\%$ of that sample exceeded the 95% significance contour, in agreement with expectations. It is therefore the inclusion of the observations made in the first 23 days of *October*, 1994 *alone* that contributes the higher than expected number of images exceeding the 95% significance contour. The increase to 9.5% is in the cumulative total; some $\sim 30\%$ of the images taken in the first 23 days of *October*, 1994 exceed the 95% level of significance. The onset of DN159 corruption therefore appears to have occurred in the 23 days preceding its discovery in engineering telemetry on $24^{th} October, 1994$.

5   THE 18th AND 19th EPISODES

The test for DN159 corruption outlined in Section 3.3 was applied to all observations made between $1^{st} October, 1994$ and $27^{th} September, 1996$, that is to the entire 18th and 19th observing episodes. In total, 1895 images are identified as affected by the DMU anomaly at the 3σ level. The results are summarised in Table 2. Some 5% of Vilspa SWP images, and 11% of Goddard SWP images from the 18th episode are classified as corrupt. The higher frequency of corruption in the Goddard images may reflect a greater probability of corruption occurring in the US2 (high radiation background) shift, although this has not been investigated in detail.

The corruption ratio, r_c, is defined by $r_c = C_{159}/O_{159}$, where $0 \le r_c \le 1$. The distribution of r_c for SWP images is illustrated in Figure 6. The dominant peak in this distribution for 19th episode images largely reflects a population of highly corrupted images, $(r_c \to 1)$, taken mostly during monitoring campaigns, when exposure times were selected to optimise the detection of weaker spectral features, and efforts to contain the DMU anomaly were relaxed. Figure 6 also illustrates the evolution of the DMU anomaly; not only was the

7

Table 2: *Summary of DN159 3σ-corruption tests.*

Station	Episode	Camera	Images	Corrupt
Goddard	18	LWP	1736	96
		SWP	2675	289
Vilspa		LWP	515	25
		SWP	1069	50
Vilspa	19	LWP	1150	417
		SWP	2361	1018

frequency of corruption greater in the 19th episode than in the 18th episode, but the *degree* of corruption also tended to be greater.

6   DISCUSSION

The possibility of distinguishing corrupt and non-corrupt DN159 pixels was investigated by taking several images from before the onset of corruption, and randomly replacing pixels in the range $DN(160 - 191)$ with DN159. Efforts were then made to distinguish these artificially corrupted pixels from uncorrupted DN159 pixels by comparing their residuals from taut spline fits both along and orthogonal to the dispersion direction, to the general rms scatter about these fits. The success rate was sufficiently low to lead to this approach being abandoned as unsuited to a homogeneous archive of processed images. Instead, a more conservative approach is adopted of assigning to *every* DN159 pixel in a corrupt raw image an abnormality flag (-8). For flux extraction by NEWSIPS, this flag is treated according to the rules governing propagation of abnormality flags, as described in the NEWSIPS manual (Chapter 9). For flux extraction in INES, each DN159 pixel in the corrupt raw image is given zero weight in the extraction procedure. The keyword ABNOTHER in the FITS header of all such spectra is set to 'DMU', and the header COMMENTS section includes a warning that the image is affected by the DMU anomaly. The total number of DN159 pixels in the science image, the most probable number of corrupted pixels and its uncertainty is also given. For convenience, this information is summarized in the Appendix.

ACKNOWLEDGMENTS
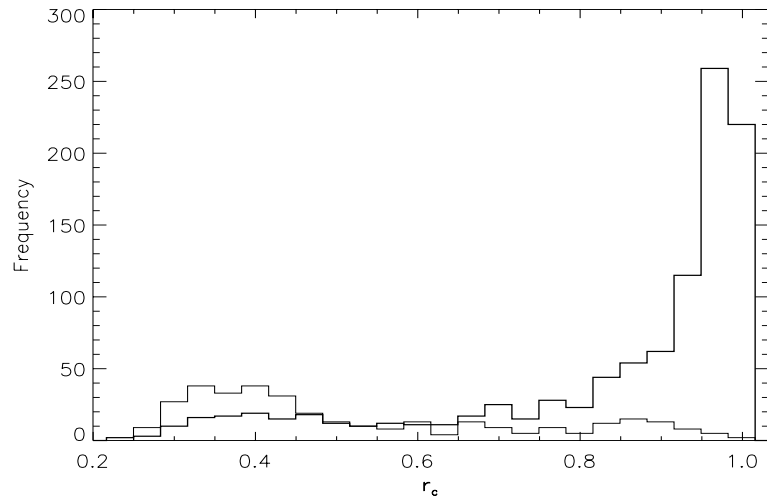
Figure 6: *Distributions of the corruption ratio, r_c, for 18th episode (thin line) and 19th episode (heavy line) SWP images.*

References

Pérez-Calpena A., Pepoy J., 1997, Final Report IUE-Spacecraft Operations, ESA SP-1215, 61, INES Document 2.7.4

Appendix

Table 3 is a summary of the 1357 3σ-corrupted SWP images, and lists for each image the number of DN159 pixels in the science image, O_{159}, the most probable number of corrupt DN159 pixels, C_{159}, and its confidence interval (θ_l, θ_u), which corresponds to $C_{159}\,{}^{\theta_u}_{\theta_l}$.

Table 4 is the corresponding summary of the 538 3σ-corrupted LWP images.

Table 3

Image	O_{159}	C_{159}	θ_u	θ_l	Image	O_{159}	C_{159}	θ_u	θ_l
SWP52335	144	130	9	-9	SWP53470	363	170	41	-41
SWP52352	136	46	15	-15	SWP53471	262	104	32	-32
SWP52502	275	128	39	-39	SWP53472	41	25	7	-7
SWP52511	237	75	23	-23	SWP53473	325	84	28	-28
SWP52525	296	108	37	-37	SWP53474	271	101	31	-31
SWP52557	244	102	31	-31	SWP53492	273	86	27	-27
SWP52567	241	93	31	-31	SWP53495	279	95	30	-30
SWP52728	328	120	40	-40	SWP53497	340	104	33	-33
SWP52836	82	74	3	-4	SWP53500	368	152	36	-36
SWP52837	37	32	3	-3	SWP53503	588	349	28	-28
SWP52864	228	87	28	-28	SWP53522	258	92	31	-31
SWP52912	88	38	9	-9	SWP53528	295	108	26	-26
SWP52951	52	32	4	-4	SWP53530	343	143	43	-43
SWP53012	232	162	42	-42	SWP53533	662	434	32	-32
SWP53070	83	35	11	-11	SWP53549	271	113	33	-33
SWP53161	83	75	6	-6	SWP53554	341	122	35	-35
SWP53215	126	85	12	-12	SWP53555	287	119	33	-33
SWP53315	349	90	27	-27	SWP53557	340	145	38	-38
SWP53382	341	132	39	-39	SWP53560	366	158	41	-41
SWP53385	341	142	39	-39	SWP53573	262	79	25	-25
SWP53388	328	106	30	-30	SWP53578	341	117	34	-34
SWP53392	267	96	32	-32	SWP53587	331	88	28	-28
SWP53394	349	123	35	-35	SWP53589	45	18	6	-6
SWP53400	341	101	34	-34	SWP53590	338	151	42	-42
SWP53413	271	105	31	-31	SWP53591	273	78	25	-25
SWP53416	270	85	26	-26	SWP53614	332	127	37	-37
SWP53421	335	146	43	-43	SWP53615	273	108	33	-33
SWP53424	341	128	38	-38	SWP53647	327	112	38	-38
SWP53443	270	117	37	-37	SWP53663	319	100	33	-33
SWP53445	342	111	34	-34	SWP53664	257	76	26	-26
SWP53448	336	105	32	-32	SWP53667	274	107	32	-32
SWP53454	327	109	33	-33	SWP53687	370	161	34	-34
SWP53467	339	144	39	-39	SWP53690	340	138	38	-38

Table 3 continued

Image	O_{159}	C_{159}	θ_u	θ_l	Image	O_{159}	C_{159}	θ_u	θ_l
SWP53691	288	130	32	-32	SWP54173	295	109	33	-33
SWP53692	34	16	6	-6	SWP54182	172	73	22	-22
SWP53694	278	116	32	-32	SWP54183	195	65	21	-21
SWP53696	338	105	35	-35	SWP54186	51	45	5	-5
SWP53712	265	92	30	-30	SWP54187	194	78	23	-23
SWP53718	265	77	25	-25	SWP54188	238	77	25	-25
SWP53720	336	115	35	-35	SWP54189	295	181	17	-17
SWP53723	359	147	38	-38	SWP54192	491	183	54	-54
SWP53741	311	123	40	-40	SWP54193	22	14	3	-4
SWP53742	275	114	33	-33	SWP54194	198	75	25	-25
SWP53743	41	19	5	-5	SWP54224	235	68	22	-22
SWP53747	336	133	42	-42	SWP54237	24	16	3	-4
SWP53750	314	132	40	-40	SWP54241	257	103	25	-25
SWP53753	364	158	38	-38	SWP54282	40	35	1	-2
SWP53754	247	84	22	-22	SWP54283	45	43	2	-3
SWP53772	269	75	20	-20	SWP54284	151	49	13	-13
SWP53775	264	95	30	-30	SWP54348	218	82	22	-22
SWP53783	370	152	36	-36	SWP54349	742	545	24	-24
SWP53829	139	73	22	-22	SWP54362	284	85	26	-26
SWP53831	7	6	1	-2	SWP54366	261	104	24	-24
SWP53833	195	89	22	-22	SWP54367	345	167	26	-26
SWP53919	289	101	34	-34	SWP54368	332	176	29	-29
SWP53920	321	85	28	-28	SWP54370	418	181	37	-37
SWP53921	341	145	39	-39	SWP54372	324	121	39	-39
SWP53922	363	126	33	-33	SWP54386	2171	823	257	-257
SWP53923	286	107	32	-32	SWP54393	368	144	37	-37
SWP53926	41	22	7	-7	SWP54409	350	114	35	-35
SWP53943	442	146	46	-46	SWP54417	336	139	37	-37
SWP53961	181	161	15	-15	SWP54420	254	102	26	-26
SWP53963	16289	14442	239	-239	SWP54422	317	117	35	-35
SWP53964	8391	7354	110	-110	SWP54424	382	126	40	-40
SWP53989	296	115	36	-36	SWP54425	471	247	53	-53
SWP53991	299	91	29	-29	SWP54427	173	48	16	-16
SWP54035	114	49	13	-13	SWP54500	147	112	30	-30
SWP54053	234	88	23	-23	SWP54540	157	50	15	-15
SWP54116	21	12	4	-5	SWP54596	394	129	39	-39
SWP54130	690	271	87	-87	SWP54598	483	168	51	-51
SWP54133	254	77	23	-23	SWP54599	649	238	70	-70
SWP54134	264	92	26	-26	SWP54601	444	215	54	-54
SWP54135	17	14	2	-3	SWP54602	399	169	35	-35
SWP54157	254	70	23	-23	SWP54603	433	197	35	-35

Table 3 continued

Image	O_{159}	C_{159}	θ_u	θ_l	Image	O_{159}	C_{159}	θ_u	θ_l
SWP54604	701	499	37	-37	SWP55497	19126	18457	144	-144
SWP54626	647	531	30	-30	SWP55498	18830	17040	215	-215
SWP54642	30	26	3	-4	SWP55499	18856	16791	182	-182
SWP54644	27	26	1	-3	SWP55500	23449	21913	192	-192
SWP54729	33	17	5	-5	SWP55503	166	78	21	-21
SWP54776	158	65	13	-13	SWP55504	138	70	16	-16
SWP54777	173	84	18	-18	SWP55505	309	124	34	-34
SWP54778	355	280	16	-16	SWP55507	226	88	25	-25
SWP54928	18	13	3	-4	SWP55508	78	39	11	-11
SWP54929	9	7	1	-3	SWP55510	1981	554	166	-166
SWP54930	18	17	1	-3	SWP55511	582	350	47	-47
SWP54931	9	5	1	-2	SWP55514	10442	8701	217	-217
SWP54932	19	17	1	-2	SWP55515	118	110	8	-8
SWP54933	11	9	1	-2	SWP55516	2522	984	300	-300
SWP54934	16	14	1	-3	SWP55519	2535	859	260	-260
SWP54935	19	18	1	-2	SWP55525	309	107	36	-36
SWP55026	10	7	2	-2	SWP55538	225	80	21	-21
SWP55035	204	72	24	-24	SWP55548	2529	756	242	-242
SWP55119	361	133	40	-40	SWP55549	2342	954	261	-261
SWP55121	360	124	38	-38	SWP55550	907	550	152	-152
SWP55133	372	114	35	-35	SWP55559	9705	7989	211	-211
SWP55143	381	125	38	-38	SWP55560	4034	2988	157	-157
SWP55145	388	161	48	-48	SWP55562	6565	4893	233	-233
SWP55185	33	25	2	-2	SWP55565	4097	2516	248	-248
SWP55206	16	9	3	-3	SWP55566	931	732	141	-141
SWP55208	19	12	3	-3	SWP55568	5290	3579	246	-246
SWP55273	155	68	21	-21	SWP55570	3191	2130	144	-144
SWP55429	11	9	1	-2	SWP55571	300	117	26	-26
SWP55430	8	7	1	-2	SWP55572	310	171	30	-30
SWP55434	20	17	2	-3	SWP55573	203	77	14	-14
SWP55437	6	5	1	-2	SWP55574	341	159	28	-28
SWP55438	7	6	1	-2	SWP55581	262	139	18	-18
SWP55439	9	7	1	-2	SWP55584	11210	9691	174	-174
SWP55474	388	198	20	-20	SWP55585	2285	2249	13	-13
SWP55477	61	58	2	-3	SWP55586	27231	25632	166	-166
SWP55482	250	78	25	-25	SWP55587	2882	2637	66	-66
SWP55487	327	104	30	-30	SWP55588	36698	34536	154	-154
SWP55492	1776	887	143	-143	SWP55589	38337	36167	151	-151
SWP55493	4667	3117	182	-182	SWP55590	43340	41500	132	-132
SWP55494	7991	6482	168	-168	SWP55592	24155	24008	30	-30
SWP55495	13547	12037	184	-184	SWP55593	14757	12946	191	-191

Table 3 continued

Image	O_{159}	C_{159}	θ_u	θ_l	Image	O_{159}	C_{159}	θ_u	θ_l
SWP55597	60	20	6	-6	SWP55757	140	55	16	-16
SWP55599	490	257	31	-31	SWP55767	208	94	28	-28
SWP55609	228	72	23	-23	SWP55771	44	34	8	-8
SWP55622	470	212	45	-45	SWP55777	200	85	24	-24
SWP55623	993	647	56	-56	SWP55816	204	111	16	-16
SWP55625	556	389	18	-18	SWP55841	312	123	32	-32
SWP55626	213	67	20	-20	SWP55843	171	97	17	-17
SWP55633	131	57	15	-15	SWP55844	613	432	29	-29
SWP55667	334	132	37	-37	SWP55845	347	220	15	-15
SWP55677	226	77	22	-22	SWP55846	212	118	14	-14
SWP55678	485	167	44	-44	SWP55847	221	95	15	-15
SWP55686	200	62	20	-20	SWP55848	323	199	18	-18
SWP55687	292	123	32	-32	SWP55849	180	56	17	-17
SWP55692	606	208	54	-54	SWP55850	191	58	15	-15
SWP55699	296	104	33	-33	SWP55851	356	130	25	-25
SWP55704	12	7	2	-3	SWP55852	208	100	19	-19
SWP55710	237	84	24	-24	SWP55854	465	213	21	-21
SWP55711	174	47	14	-14	SWP55856	190	80	25	-25
SWP55712	166	73	12	-12	SWP55857	316	111	30	-30
SWP55713	229	113	18	-18	SWP55858	220	102	15	-15
SWP55714	191	98	20	-20	SWP55859	219	104	15	-15
SWP55716	418	141	48	-48	SWP55860	599	398	30	-30
SWP55723	564	434	17	-17	SWP55863	355	142	29	-29
SWP55725	104	69	7	-7	SWP55864	183	63	19	-19
SWP55726	1835	1564	39	-39	SWP55866	189	61	20	-20
SWP55727	1666	1340	48	-48	SWP55868	368	245	23	-23
SWP55729	159	117	16	-16	SWP55869	268	152	23	-23
SWP55730	242	128	18	-18	SWP55870	416	290	18	-18
SWP55731	168	75	17	-17	SWP55871	271	138	23	-23
SWP55732	152	53	17	-17	SWP55872	261	138	17	-17
SWP55735	319	93	29	-29	SWP55873	348	235	24	-24
SWP55738	178	72	20	-20	SWP55874	297	158	25	-25
SWP55743	52	37	6	-6	SWP55875	588	445	17	-17
SWP55744	600	502	15	-15	SWP55876	504	388	21	-21
SWP55745	652	536	17	-17	SWP55877	282	135	21	-21
SWP55746	194	100	12	-12	SWP55878	530	418	18	-18
SWP55747	31	26	3	-4	SWP55879	915	799	18	-18
SWP55752	190	119	12	-12	SWP55880	176	67	18	-18
SWP55753	173	54	13	-13	SWP55881	163	76	19	-19
SWP55754	278	131	16	-16	SWP55882	163	69	18	-18
SWP55756	297	177	26	-26	SWP55884	161	63	17	-17

Table 3 continued

Image	O_{159}	C_{159}	θ_u	θ_l	Image	O_{159}	C_{159}	θ_u	θ_l
SWP55885	227	81	19	-19	SWP56160	69	65	2	-3
SWP55886	207	79	14	-14	SWP56162	12	11	1	-2
SWP55887	239	122	19	-19	SWP56163	194	188	3	-4
SWP55888	329	200	31	-31	SWP56164	25	24	1	-3
SWP55889	190	80	20	-20	SWP56169	19	18	1	-2
SWP55890	343	208	12	-12	SWP56170	25	22	2	-3
SWP55891	429	305	18	-18	SWP56176	313	193	22	-22
SWP55892	460	357	26	-26	SWP56177	309	168	14	-14
SWP55893	344	211	19	-19	SWP56179	755	426	53	-53
SWP55896	369	154	27	-27	SWP56180	829	421	42	-42
SWP55906	955	831	20	-20	SWP56181	1765	1392	59	-59
SWP55912	10	9	1	-3	SWP56184	551	216	46	-46
SWP55913	318	219	18	-18	SWP56185	825	471	45	-45
SWP55957	20	18	2	-4	SWP56188	267	127	26	-26
SWP55959	1114	343	101	-101	SWP56199	213	84	21	-21
SWP55964	26	22	4	-5	SWP56200	272	102	31	-31
SWP55979	288	193	16	-16	SWP56201	279	100	29	-29
SWP55981	128	71	14	-14	SWP56208	46	25	7	-7
SWP55986	80	38	11	-11	SWP56210	38	33	3	-4
SWP55988	240	81	25	-25	SWP56216	17	13	2	-3
SWP55990	202	67	22	-22	SWP56218	14	11	3	-4
SWP55993	14	13	1	-2	SWP56221	16	14	1	-2
SWP55998	353	114	37	-37	SWP56224	27	24	2	-3
SWP55999	561	198	61	-61	SWP56228	218	169	40	-40
SWP56006	12	10	1	-2	SWP56238	342	224	29	-29
SWP56016	188	168	15	-15	SWP56239	665	516	21	-21
SWP56017	553	375	32	-32	SWP56241	29	26	2	-3
SWP56036	149	125	20	-20	SWP56242	7	6	1	-1
SWP56041	204	192	6	-6	SWP56243	17	10	2	-2
SWP56047	14	12	1	-3	SWP56244	64	62	2	-4
SWP56061	1998	656	213	-213	SWP56245	35	33	1	-2
SWP56063	893	621	44	-44	SWP56246	93	90	2	-4
SWP56071	622	189	57	-57	SWP56250	556	422	18	-18
SWP56083	19	15	2	-3	SWP56255	19	18	1	-2
SWP56088	16	11	2	-3	SWP56257	605	599	3	-4
SWP56113	530	197	55	-55	SWP56290	57	48	4	-4
SWP56127	1248	394	120	-120	SWP56294	17	12	3	-4
SWP56138	21	15	3	-4	SWP56304	33	28	2	-3
SWP56139	25	24	1	-3	SWP56332	19	17	1	-2
SWP56140	15	14	1	-2	SWP56337	478	347	20	-20
SWP56142	388	375	4	-4	SWP56338	52	40	5	-5

Table 3 continued

Image	O_{159}	C_{159}	θ_u	θ_l	Image	O_{159}	C_{159}	θ_u	θ_l
SWP56343	64	41	7	-7	SWP56548	275	88	28	-28
SWP56354	23	12	4	-4	SWP56549	298	114	31	-31
SWP56355	51	42	4	-4	SWP56550	278	95	30	-30
SWP56358	1901	877	134	-134	SWP56551	274	98	31	-31
SWP56371	57	44	5	-5	SWP56553	311	112	31	-31
SWP56374	544	253	62	-62	SWP56554	334	130	29	-29
SWP56377	20	11	3	-4	SWP56571	313	93	18	-18
SWP56381	37	35	1	-2	SWP56572	348	171	33	-33
SWP56387	9	7	1	-2	SWP56573	289	104	30	-30
SWP56388	12	10	1	-2	SWP56576	285	93	27	-27
SWP56396	90	72	7	-7	SWP56578	306	87	29	-29
SWP56408	237	68	23	-23	SWP56582	643	567	53	-53
SWP56409	39	18	5	-5	SWP56590	261	90	28	-28
SWP56410	37	14	5	-5	SWP56594	412	218	26	-26
SWP56411	17	13	4	-5	SWP56595	639	458	29	-29
SWP56432	262	77	26	-26	SWP56596	880	724	32	-32
SWP56441	285	62	20	-20	SWP56597	481	294	26	-26
SWP56444	282	78	26	-26	SWP56598	1777	1600	26	-26
SWP56445	297	104	31	-31	SWP56599	270	105	34	-34
SWP56447	302	106	27	-27	SWP56600	270	105	33	-33
SWP56454	17	15	2	-4	SWP56612	309	154	32	-32
SWP56461	276	72	19	-19	SWP56614	295	114	30	-30
SWP56464	292	114	30	-30	SWP56615	481	322	35	-35
SWP56469	270	95	31	-31	SWP56616	282	135	36	-36
SWP56477	300	95	28	-28	SWP56617	307	142	31	-31
SWP56496	266	73	24	-24	SWP56618	960	806	35	-35
SWP56498	292	106	31	-31	SWP56619	1092	900	26	-26
SWP56502	272	78	24	-24	SWP56620	587	414	30	-30
SWP56505	290	88	26	-26	SWP56625	709	516	27	-27
SWP56506	263	111	34	-34	SWP56633	64	57	3	-4
SWP56507	262	90	30	-30	SWP56635	7	5	1	-2
SWP56510	284	83	26	-26	SWP56638	14	10	2	-2
SWP56511	300	101	31	-31	SWP56640	55	52	2	-3
SWP56514	302	102	29	-29	SWP56643	23	19	2	-3
SWP56515	299	103	25	-25	SWP56648	13	10	2	-3
SWP56532	310	124	27	-27	SWP56649	10	7	2	-3
SWP56533	360	172	30	-30	SWP56655	23	18	2	-3
SWP56535	279	92	29	-29	SWP56656	28	23	2	-3
SWP56540	288	103	29	-29	SWP56664	15	14	1	-2
SWP56541	292	113	31	-31	SWP56666	317	305	5	-5
SWP56544	295	93	28	-28	SWP56668	16	10	3	-4

Table 3 continued

Image	O_{159}	C_{159}	θ_u	θ_l	Image	O_{159}	C_{159}	θ_u	θ_l
SWP56669	15	9	3	-4	SWP56875	983	771	35	-35
SWP56675	38	35	1	-2	SWP56881	893	780	16	-16
SWP56677	1087	947	23	-23	SWP56887	37	31	4	-5
SWP56688	16	12	3	-5	SWP56888	79	64	5	-5
SWP56699	279	179	18	-18	SWP56899	1652	1624	25	-25
SWP56703	347	260	16	-16	SWP56900	3758	3708	27	-27
SWP56731	39	35	3	-3	SWP56907	2433	976	249	-249
SWP56762	8	7	1	-2	SWP56914	6	4	1	-2
SWP56775	538	334	33	-33	SWP56915	12	11	1	-2
SWP56777	717	618	17	-17	SWP56922	14	10	2	-2
SWP56778	23	19	3	-4	SWP56934	76	51	8	-8
SWP56790	1163	832	31	-31	SWP56935	91	77	6	-6
SWP56795	444	212	30	-30	SWP56938	31	18	5	-5
SWP56796	412	194	35	-35	SWP56939	164	94	13	-13
SWP56797	338	143	40	-40	SWP56943	122	56	13	-13
SWP56798	362	133	35	-35	SWP56948	119	48	13	-13
SWP56803	870	676	38	-38	SWP56957	120	51	14	-14
SWP56810	417	187	55	-55	SWP56962	115	47	12	-12
SWP56813	196	93	27	-27	SWP56963	83	60	6	-6
SWP56816	89	82	4	-4	SWP56964	58	32	7	-7
SWP56818	2308	2227	20	-20	SWP56969	41	30	6	-6
SWP56819	90	75	7	-7	SWP56970	38	33	3	-3
SWP56820	193	86	24	-24	SWP56978	46	44	2	-3
SWP56822	176	68	22	-22	SWP56985	30	27	2	-3
SWP56824	1923	1816	19	-19	SWP56989	215	115	18	-18
SWP56825	246	212	9	-9	SWP56990	5744	4048	210	-210
SWP56828	272	89	24	-24	SWP56992	42	36	3	-4
SWP56829	303	141	27	-27	SWP56994	18	15	1	-2
SWP56830	508	342	28	-28	SWP56995	14521	12653	195	-195
SWP56831	1426	1218	30	-30	SWP57001	7634	6482	205	-205
SWP56838	46	36	4	-4	SWP57005	17	14	2	-3
SWP56841	59	43	15	-15	SWP57009	19198	17607	210	-210
SWP56849	34	25	8	-8	SWP57020	11667	10036	221	-221
SWP56858	781	538	46	-46	SWP57025	30	21	8	-8
SWP56860	179	164	10	-10	SWP57029	84	72	5	-5
SWP56864	332	147	31	-31	SWP57036	2505	2245	20	-20
SWP56865	47	41	4	-4	SWP57037	85	43	7	-7
SWP56868	16	15	1	-2	SWP57040	355	175	33	-33
SWP56869	582	574	4	-4	SWP57045	1335	1183	18	-18
SWP56870	250	108	31	-31	SWP57048	422	249	18	-18
SWP56874	16	12	3	-4	SWP57050	161	107	7	-7

Table 3 continued

Image	O_{159}	C_{159}	θ_u	θ_l	Image	O_{159}	C_{159}	θ_u	θ_l
SWP57051	2007	1871	18	-18	SWP57116	32	30	2	-3
SWP57052	447	307	18	-18	SWP57117	437	281	23	-23
SWP57054	114	87	7	-7	SWP57119	100	50	10	-10
SWP57056	262	98	18	-18	SWP57121	1715	1576	24	-24
SWP57057	43	40	2	-4	SWP57122	32	29	2	-3
SWP57058	303	279	14	-14	SWP57124	271	133	22	-22
SWP57059	3740	3641	20	-20	SWP57126	158	96	10	-10
SWP57060	346	183	19	-19	SWP57128	483	321	17	-17
SWP57062	161	118	15	-15	SWP57130	232	205	13	-13
SWP57063	136	128	3	-4	SWP57132	1822	1701	23	-23
SWP57064	1312	1143	17	-17	SWP57133	32	28	3	-4
SWP57065	19	18	2	-4	SWP57134	207	72	22	-22
SWP57066	498	466	17	-17	SWP57140	309	155	21	-21
SWP57067	435	314	25	-25	SWP57142	154	96	12	-12
SWP57068	381	250	22	-22	SWP57143	229	191	11	-11
SWP57070	111	49	9	-9	SWP57144	1716	1546	28	-28
SWP57071	85	45	7	-7	SWP57145	1815	1682	22	-22
SWP57073	149	115	12	-12	SWP57147	221	72	23	-23
SWP57076	1587	1467	26	-26	SWP57153	151	103	12	-12
SWP57078	267	126	26	-26	SWP57155	1242	1099	22	-22
SWP57080	88	37	10	-10	SWP57156	390	345	11	-11
SWP57083	401	260	27	-27	SWP57158	928	782	24	-24
SWP57085	143	99	14	-14	SWP57159	212	151	5	-5
SWP57086	1339	1186	20	-20	SWP57162	622	467	25	-25
SWP57087	229	99	29	-29	SWP57163	304	247	11	-11
SWP57088	15	11	3	-3	SWP57165	1494	1376	27	-27
SWP57089	128	76	15	-15	SWP57166	449	413	15	-15
SWP57092	482	333	24	-24	SWP57168	1249	1127	20	-20
SWP57093	25	20	2	-3	SWP57169	220	180	12	-12
SWP57095	1395	1247	22	-22	SWP57172	868	730	22	-22
SWP57096	243	88	26	-26	SWP57173	191	147	11	-11
SWP57098	96	42	11	-11	SWP57174	23	20	2	-3
SWP57101	60	35	10	-10	SWP57176	2016	1898	22	-22
SWP57103	152	93	8	-8	SWP57177	280	145	28	-28
SWP57105	1923	1765	17	-17	SWP57178	139	77	10	-10
SWP57107	294	135	21	-21	SWP57181	335	181	26	-26
SWP57109	104	45	9	-9	SWP57182	171	112	13	-13
SWP57111	441	297	25	-25	SWP57183	19	18	1	-3
SWP57112	15	13	2	-4	SWP57185	2042	1915	21	-21
SWP57113	292	235	10	-10	SWP57186	631	595	9	-9
SWP57115	2052	1943	25	-25	SWP57187	247	109	24	-24

Table 3 continued

Image	O_{159}	C_{159}	θ_u	θ_l	Image	O_{159}	C_{159}	θ_u	θ_l
SWP57192	502	354	21	-21	SWP57250	35	34	1	-3
SWP57193	231	184	13	-13	SWP57251	2671	2549	15	-15
SWP57194	22	19	2	-3	SWP57252	148	97	14	-14
SWP57195	1544	1399	16	-16	SWP57253	617	494	27	-27
SWP57196	481	437	14	-14	SWP57254	144	90	12	-12
SWP57197	51	47	3	-4	SWP57256	25	15	4	-5
SWP57198	241	89	23	-23	SWP57257	19	14	3	-4
SWP57199	109	55	14	-14	SWP57258	204	66	16	-16
SWP57202	334	172	24	-24	SWP57259	108	64	14	-14
SWP57203	95	54	15	-15	SWP57260	25	24	1	-3
SWP57204	30	25	2	-3	SWP57261	1923	1767	23	-23
SWP57206	1152	1016	22	-22	SWP57263	2530	2429	25	-25
SWP57207	300	245	9	-9	SWP57264	242	100	23	-23
SWP57208	30	29	1	-3	SWP57265	93	37	12	-12
SWP57209	145	140	1	-3	SWP57268	276	112	22	-22
SWP57210	35	30	2	-4	SWP57270	226	170	11	-11
SWP57211	261	119	20	-20	SWP57272	430	286	24	-24
SWP57215	258	116	22	-22	SWP57273	91	40	7	-7
SWP57216	154	89	11	-11	SWP57276	1942	1788	19	-19
SWP57219	1239	1129	24	-24	SWP57277	463	411	12	-12
SWP57220	543	486	10	-10	SWP57278	15	13	1	-2
SWP57221	237	97	24	-24	SWP57280	649	518	24	-24
SWP57225	316	176	28	-28	SWP57281	188	149	13	-13
SWP57226	137	83	14	-14	SWP57284	698	526	14	-14
SWP57227	11	9	1	-2	SWP57285	181	127	9	-9
SWP57229	1381	1214	17	-17	SWP57286	10	8	1	-2
SWP57230	543	483	10	-10	SWP57289	1530	1420	20	-20
SWP57231	1209	1050	17	-17	SWP57290	389	370	16	-16
SWP57232	366	319	11	-11	SWP57291	14	13	1	-3
SWP57235	1476	1332	22	-22	SWP57293	2004	1876	19	-19
SWP57236	488	440	13	-13	SWP57294	354	312	8	-8
SWP57237	16	12	2	-4	SWP57295	23	22	1	-3
SWP57238	2698	2566	18	-18	SWP57297	482	334	20	-20
SWP57239	658	626	16	-16	SWP57298	131	92	10	-10
SWP57240	34	33	1	-3	SWP57299	20	17	2	-4
SWP57242	2011	1880	19	-19	SWP57302	1280	1158	20	-20
SWP57243	459	419	10	-10	SWP57303	277	240	14	-14
SWP57244	22	20	1	-3	SWP57304	12	11	1	-3
SWP57246	1305	1160	20	-20	SWP57305	24	23	1	-2
SWP57247	340	291	10	-10	SWP57306	523	502	7	-7
SWP57249	26	24	1	-2	SWP57307	1836	1733	22	-22

Table 3 continued

Image	O_{159}	C_{159}	θ_u	θ_l	Image	O_{159}	C_{159}	θ_u	θ_l
SWP57308	2227	2111	16	-16	SWP57620	37	25	3	-4
SWP57309	1719	1598	20	-20	SWP57621	52	46	5	-5
SWP57310	327	301	13	-13	SWP57622	111	104	6	-6
SWP57311	12	11	1	-2	SWP57623	313	307	4	-5
SWP57313	2622	2496	16	-16	SWP57624	184	177	4	-5
SWP57314	416	371	9	-9	SWP57625	189	181	3	-4
SWP57315	11	10	1	-2	SWP57626	252	244	3	-4
SWP57316	1838	1694	15	-15	SWP57627	254	248	3	-4
SWP57317	228	193	7	-7	SWP57628	180	173	4	-4
SWP57319	659	520	22	-22	SWP57629	178	170	5	-6
SWP57320	146	114	11	-11	SWP57630	187	181	5	-5
SWP57321	12	11	1	-2	SWP57631	93	82	4	-4
SWP57325	838	686	22	-22	SWP57632	212	205	5	-6
SWP57326	195	168	14	-14	SWP57633	249	242	5	-5
SWP57327	8	6	1	-2	SWP57634	405	399	4	-5
SWP57328	1312	1174	23	-23	SWP57635	312	307	3	-4
SWP57329	280	240	10	-10	SWP57636	365	360	3	-4
SWP57330	37	33	2	-3	SWP57637	317	312	3	-4
SWP57332	19	18	1	-2	SWP57638	394	388	3	-3
SWP57333	458	450	6	-7	SWP57639	376	371	3	-4
SWP57339	117	52	11	-11	SWP57640	385	379	3	-4
SWP57345	369	200	28	-28	SWP57641	360	355	4	-4
SWP57351	19	12	4	-4	SWP57642	370	363	2	-3
SWP57352	19	11	3	-4	SWP57643	390	383	3	-4
SWP57360	36	34	1	-2	SWP57644	360	352	2	-2
SWP57361	58	57	1	-3	SWP57645	260	254	2	-3
SWP57365	61	52	7	-7	SWP57646	301	295	3	-3
SWP57367	653	365	42	-42	SWP57647	336	330	4	-5
SWP57370	29	28	1	-3	SWP57648	324	318	4	-5
SWP57374	2331	561	179	-179	SWP57649	277	269	4	-4
SWP57377	6624	4459	167	-167	SWP57650	313	307	4	-5
SWP57378	17848	15867	216	-216	SWP57652	370	362	4	-5
SWP57392	32	27	3	-3	SWP57653	437	430	4	-5
SWP57393	2001	1722	32	-32	SWP57654	450	443	3	-3
SWP57394	550	265	37	-37	SWP57655	447	440	2	-3
SWP57403	18	17	1	-2	SWP57656	440	436	3	-4
SWP57434	11	10	1	-2	SWP57657	464	458	3	-3
SWP57453	14	13	1	-2	SWP57658	474	468	4	-5
SWP57460	9	8	1	-2	SWP57659	460	454	3	-4
SWP57478	7	6	1	-2	SWP57660	417	411	3	-4
SWP57479	12	11	1	-3	SWP57661	387	381	3	-4

Table 3 continued

Image	O_{159}	C_{159}	θ_u	θ_l	Image	O_{159}	C_{159}	θ_u	θ_l
SWP57662	398	392	3	-4	SWP57704	425	419	5	-6
SWP57663	348	342	3	-3	SWP57705	463	459	4	-4
SWP57664	245	236	3	-3	SWP57706	450	445	3	-4
SWP57666	312	306	4	-5	SWP57707	392	387	4	-4
SWP57667	309	302	3	-4	SWP57708	435	431	4	-5
SWP57668	389	384	4	-5	SWP57709	455	448	2	-3
SWP57669	439	432	4	-5	SWP57710	432	425	3	-3
SWP57670	416	409	2	-3	SWP57711	474	470	3	-4
SWP57671	434	428	4	-5	SWP57712	411	404	2	-2
SWP57672	460	456	3	-4	SWP57713	475	470	5	-6
SWP57673	435	429	5	-6	SWP57714	438	432	3	-4
SWP57674	435	430	4	-4	SWP57715	406	400	4	-5
SWP57675	401	395	5	-7	SWP57716	371	366	4	-5
SWP57676	423	415	3	-3	SWP57717	397	390	3	-4
SWP57677	437	430	3	-4	SWP57718	436	432	4	-5
SWP57678	465	460	4	-5	SWP57719	415	411	4	-5
SWP57679	402	395	3	-4	SWP57720	304	300	4	-5
SWP57680	370	362	3	-4	SWP57721	337	332	4	-5
SWP57681	413	407	3	-4	SWP57722	388	382	4	-5
SWP57682	391	385	4	-5	SWP57723	474	467	2	-3
SWP57683	509	502	4	-5	SWP57724	440	435	3	-4
SWP57684	451	444	5	-6	SWP57725	44	43	1	-2
SWP57685	476	471	3	-4	SWP57736	30	29	1	-2
SWP57686	441	437	3	-4	SWP57737	668	662	4	-5
SWP57687	454	449	4	-4	SWP57738	73	72	1	-3
SWP57688	376	370	4	-4	SWP57740	66	65	1	-3
SWP57689	421	416	3	-4	SWP57741	48	46	1	-4
SWP57690	407	401	4	-4	SWP57742	73	72	1	-3
SWP57691	447	441	3	-3	SWP57743	65	64	1	-2
SWP57692	441	436	4	-5	SWP57744	73	72	1	-2
SWP57693	440	427	3	-3	SWP57745	73	72	1	-3
SWP57694	488	481	3	-4	SWP57746	52	51	1	-3
SWP57695	422	417	3	-4	SWP57747	153	116	6	-6
SWP57696	443	439	3	-4	SWP57749	674	637	17	-17
SWP57697	471	466	3	-4	SWP57751	819	774	14	-14
SWP57698	452	446	4	-6	SWP57753	913	892	19	-19
SWP57699	461	454	3	-3	SWP57755	2226	2184	22	-22
SWP57700	464	459	4	-4	SWP57757	1989	1928	15	-15
SWP57701	441	437	4	-5	SWP57759	1904	1808	13	-13
SWP57702	452	447	4	-6	SWP57761	42957	40548	151	-151
SWP57703	455	448	3	-3	SWP57764	49	47	1	-2

Table 3 continued

Image	O_{159}	C_{159}	θ_u	θ_l	Image	O_{159}	C_{159}	θ_u	θ_l
SWP57766	50	48	1	-2	SWP57885	44	42	1	-2
SWP57768	67	66	1	-3	SWP57886	42	40	1	-2
SWP57770	70	69	1	-2	SWP57887	46	44	2	-3
SWP57778	48	43	2	-3	SWP57888	44	42	2	-3
SWP57779	69	66	2	-3	SWP57889	26	25	1	-3
SWP57791	389	159	40	-40	SWP57890	51	49	1	-2
SWP57793	531	192	44	-44	SWP57891	39	37	1	-2
SWP57795	7069	5233	262	-262	SWP57892	33	32	1	-2
SWP57796	3272	1620	274	-274	SWP57893	33	31	1	-1
SWP57800	3371	1580	286	-286	SWP57894	58	57	1	-2
SWP57845	12	9	1	-2	SWP57895	45	44	1	-2
SWP57847	10	7	2	-3	SWP57896	96	94	1	-2
SWP57853	21	19	1	-2	SWP57897	98	97	1	-2
SWP57854	42	41	1	-3	SWP57898	84	82	1	-2
SWP57855	41	39	1	-2	SWP57899	97	94	2	-3
SWP57856	55	54	1	-2	SWP57901	33	31	1	-2
SWP57857	44	43	1	-2	SWP57902	30	29	1	-2
SWP57858	6	4	1	-2	SWP57903	31	29	1	-2
SWP57859	10	9	1	-2	SWP57904	41	39	1	-2
SWP57860	15	14	1	-2	SWP57905	40	38	1	-2
SWP57861	31	30	1	-2	SWP57906	43	42	1	-3
SWP57862	23	22	1	-2	SWP57907	33	32	1	-3
SWP57863	6	5	1	-2	SWP57908	46	45	1	-2
SWP57864	11	9	1	-2	SWP57909	65	64	1	-2
SWP57865	12	11	1	-2	SWP57910	50	49	1	-3
SWP57867	9	7	1	-3	SWP57912	16	15	1	-2
SWP57869	13	9	2	-3	SWP57913	23	22	1	-2
SWP57870	14	11	2	-4	SWP57914	24	22	1	-2
SWP57871	23	20	2	-3	SWP57915	28	27	1	-2
SWP57872	30	28	2	-4	SWP57916	33	31	1	-1
SWP57873	25	22	2	-3	SWP57917	46	45	1	-2
SWP57874	34	32	2	-3	SWP57918	25	24	1	-2
SWP57875	29	27	2	-3	SWP57919	40	39	1	-2
SWP57876	62	57	2	-3	SWP57920	44	43	1	-2
SWP57877	58	55	2	-3	SWP57921	32	31	1	-2
SWP57878	62	58	2	-2	SWP57922	40	39	1	-3
SWP57879	49	46	2	-4	SWP57923	11	10	1	-3
SWP57880	51	48	2	-3	SWP57924	21	18	2	-3
SWP57882	67	65	2	-3	SWP57925	31	29	2	-3
SWP57883	17	15	1	-3	SWP57926	29	25	2	-3
SWP57884	30	29	1	-3	SWP57927	37	34	2	-3

Table 3 continued

Image	O_{159}	C_{159}	θ_u	θ_l	Image	O_{159}	C_{159}	θ_u	θ_l
SWP57928	39	36	2	-3	SWP57987	28	26	1	-3
SWP57929	45	42	2	-3	SWP57988	48	46	1	-2
SWP57930	54	52	2	-3	SWP57989	47	45	2	-3
SWP57931	44	42	2	-3	SWP57990	42	38	3	-4
SWP57932	59	56	2	-4	SWP57991	54	51	1	-2
SWP57933	65	63	1	-2	SWP57992	68	65	1	-2
SWP57934	69	67	1	-3	SWP57993	85	83	1	-3
SWP57935	82	81	1	-3	SWP57994	70	69	1	-3
SWP57936	73	71	1	-2	SWP57995	78	76	1	-2
SWP57937	76	73	1	-2	SWP57996	83	81	1	-2
SWP57938	82	80	2	-3	SWP57997	88	86	1	-3
SWP57939	94	91	1	-2	SWP57998	72	70	1	-3
SWP57940	100	98	1	-2	SWP57999	100	97	1	-4
SWP57941	87	86	1	-2	SWP58000	94	93	1	-3
SWP57942	110	107	2	-2	SWP58001	105	103	1	-3
SWP57945	8	5	1	-2	SWP58005	18	15	2	-3
SWP57948	12	9	1	-2	SWP58006	11	8	2	-3
SWP57949	12	9	1	-2	SWP58007	27	24	2	-3
SWP57952	18	15	1	-3	SWP58008	29	26	2	-2
SWP57953	30	27	2	-3	SWP58009	28	26	2	-3
SWP57954	43	39	2	-2	SWP58010	33	31	1	-3
SWP57955	43	37	2	-2	SWP58011	48	45	1	-2
SWP57956	54	51	2	-3	SWP58012	118	116	1	-3
SWP57957	68	65	2	-3	SWP58013	115	112	2	-3
SWP57958	77	74	2	-3	SWP58014	116	113	2	-3
SWP57959	67	63	2	-3	SWP58015	131	127	2	-2
SWP57960	84	81	2	-3	SWP58016	131	129	1	-2
SWP57961	118	115	2	-2	SWP58017	133	130	2	-3
SWP57962	104	100	2	-3	SWP58018	128	127	2	-4
SWP57969	18	15	1	-2	SWP58019	124	121	1	-2
SWP57970	31	28	2	-3	SWP58020	118	116	2	-3
SWP57971	34	32	2	-4	SWP58024	10	7	2	-3
SWP57972	38	37	1	-3	SWP58025	10	7	2	-3
SWP57978	12	10	1	-2	SWP58027	20	16	3	-3
SWP57979	74	72	1	-3	SWP58028	45	40	2	-3
SWP57980	60	58	2	-3	SWP58029	45	41	2	-3
SWP57981	67	64	1	-2	SWP58030	34	31	2	-2
SWP57983	12	9	1	-2	SWP58031	28	26	2	-3
SWP57984	15	14	2	-4	SWP58032	42	40	1	-2
SWP57985	20	18	1	-3	SWP58033	51	48	1	-2
SWP57986	29	26	2	-2	SWP58034	68	66	1	-2

Table 3 continued

Image	O_{159}	C_{159}	θ_u	θ_l	Image	O_{159}	C_{159}	θ_u	θ_l
SWP58035	55	52	2	-5	SWP58078	99	97	1	-3
SWP58036	59	57	1	-2	SWP58079	108	106	1	-2
SWP58037	81	79	1	-2	SWP58080	101	99	1	-2
SWP58038	76	74	1	-3	SWP58081	108	107	1	-3
SWP58039	91	89	1	-3	SWP58082	108	106	1	-2
SWP58040	106	103	1	-2	SWP58083	112	109	2	-4
SWP58041	136	133	2	-3	SWP58084	136	135	1	-3
SWP58042	122	119	1	-2	SWP58085	126	124	1	-3
SWP58043	127	125	2	-3	SWP58086	142	141	1	-3
SWP58044	138	136	2	-3	SWP58087	131	129	1	-2
SWP58045	55	40	12	-12	SWP58088	149	147	1	-3
SWP58046	67	65	2	-3	SWP58089	148	146	1	-2
SWP58047	92	90	2	-3	SWP58090	154	153	1	-3
SWP58048	112	109	2	-4	SWP58091	126	124	1	-2
SWP58049	99	97	2	-4	SWP58092	73	70	1	-3
SWP58050	106	103	1	-2	SWP58093	72	69	2	-3
SWP58052	122	118	1	-2	SWP58094	110	108	1	-3
SWP58053	133	130	2	-3	SWP58095	109	105	1	-2
SWP58054	119	115	1	-2	SWP58096	104	102	2	-3
SWP58055	138	135	2	-3	SWP58097	104	102	1	-3
SWP58056	146	144	2	-3	SWP58098	81	78	1	-2
SWP58057	138	136	2	-3	SWP58099	86	83	1	-2
SWP58058	137	135	2	-3	SWP58100	81	78	1	-2
SWP58059	135	133	2	-3	SWP58101	82	79	2	-2
SWP58060	108	106	1	-2	SWP58102	119	117	1	-2
SWP58061	119	118	1	-2	SWP58103	104	101	1	-2
SWP58062	138	136	1	-3	SWP58104	109	107	1	-2
SWP58063	153	152	1	-3	SWP58105	100	98	1	-3
SWP58064	139	138	1	-3	SWP58106	94	93	1	-3
SWP58065	116	114	1	-3	SWP58107	169	167	2	-4
SWP58066	116	114	1	-3	SWP58108	170	167	1	-3
SWP58067	122	120	1	-3	SWP58109	185	182	2	-2
SWP58068	124	122	1	-2	SWP58110	115	113	1	-2
SWP58070	103	101	1	-2	SWP58111	121	119	1	-2
SWP58071	86	83	1	-2	SWP58112	129	127	1	-3
SWP58072	79	77	1	-3	SWP58113	173	171	1	-2
SWP58073	77	75	1	-3	SWP58114	182	179	2	-3
SWP58074	76	74	2	-3	SWP58115	112	111	1	-2
SWP58075	80	78	2	-3	SWP58116	105	102	1	-4
SWP58076	80	78	2	-3	SWP58117	108	107	1	-2
SWP58077	84	83	1	-3	SWP58118	112	111	1	-3

Table 3 continued

Image	O_{159}	C_{159}	θ_u	θ_l	Image	O_{159}	C_{159}	θ_u	θ_l
SWP58119	111	109	1	-2	SWP58161	125	123	1	-2
SWP58120	112	110	1	-3	SWP58162	130	129	1	-3
SWP58121	108	107	1	-3	SWP58163	17	14	2	-3
SWP58122	94	93	1	-3	SWP58164	116	114	1	-2
SWP58123	115	114	1	-3	SWP58165	123	121	1	-3
SWP58124	122	120	1	-2	SWP58166	99	97	1	-3
SWP58125	169	166	1	-2	SWP58167	86	84	1	-3
SWP58126	183	181	2	-3	SWP58168	88	85	2	-4
SWP58127	174	171	2	-3	SWP58169	101	99	1	-3
SWP58128	132	131	1	-3	SWP58170	97	95	2	-3
SWP58129	120	119	1	-3	SWP58171	105	103	1	-2
SWP58130	122	120	1	-2	SWP58172	116	114	1	-3
SWP58131	149	147	1	-2	SWP58173	115	113	1	-2
SWP58132	147	145	1	-2	SWP58174	120	118	1	-2
SWP58133	130	129	1	-3	SWP58175	118	117	1	-3
SWP58134	150	149	1	-3	SWP58176	119	117	1	-2
SWP58135	134	133	1	-3	SWP58177	180	178	2	-3
SWP58136	145	143	1	-2	SWP58178	173	171	1	-3
SWP58138	79	77	1	-3	SWP58179	187	185	2	-3
SWP58139	71	69	1	-3	SWP58180	106	104	1	-2
SWP58140	135	133	1	-2	SWP58181	116	115	1	-3
SWP58141	96	95	1	-3	SWP58182	135	133	1	-2
SWP58142	102	100	1	-3	SWP58183	145	143	1	-2
SWP58143	119	116	2	-3	SWP58184	130	129	1	-3
SWP58144	136	133	2	-3	SWP58185	146	145	1	-3
SWP58145	156	154	2	-4	SWP58186	143	142	1	-3
SWP58146	103	101	1	-2	SWP58187	135	134	1	-3
SWP58147	104	102	1	-3	SWP58188	14	11	2	-3
SWP58148	95	93	2	-3	SWP58189	81	78	1	-2
SWP58149	111	109	1	-2	SWP58190	68	66	2	-3
SWP58150	105	104	1	-3	SWP58191	83	81	2	-3
SWP58151	109	108	1	-3	SWP58192	78	76	1	-2
SWP58152	120	117	2	-5	SWP58193	76	74	1	-2
SWP58153	126	125	1	-3	SWP58194	110	107	3	-4
SWP58154	120	119	1	-3	SWP58195	107	103	2	-3
SWP58155	119	117	1	-3	SWP58196	123	120	2	-3
SWP58156	178	175	1	-2	SWP58197	127	124	2	-3
SWP58157	173	171	2	-4	SWP58198	135	132	2	-3
SWP58158	182	180	2	-3	SWP58199	206	205	1	-3
SWP58159	116	115	1	-3	SWP58200	185	182	2	-3
SWP58160	123	122	1	-2	SWP58201	181	179	2	-4

Table 3 continued

Image	O_{159}	C_{159}	θ_u	θ_l	Image	O_{159}	C_{159}	θ_u	θ_l
SWP58202	112	110	1	-2	SWP58249	129	127	1	-3
SWP58203	119	117	1	-2	SWP58254	31	26	2	-3
SWP58204	125	123	1	-3	SWP58260	11	9	1	-2
SWP58205	184	182	1	-3	SWP58261	19	17	1	-2
SWP58206	203	201	2	-3	SWP58262	23	20	1	-2
SWP58207	177	175	2	-3	SWP58263	25	22	2	-3
SWP58208	195	192	1	-3	SWP58264	46	43	2	-3
SWP58209	197	195	1	-3	SWP58265	76	74	2	-3
SWP58210	233	229	3	-4	SWP58266	70	66	1	-2
SWP58211	36	34	1	-2	SWP58267	129	126	2	-3
SWP58212	15	14	1	-2	SWP58268	124	121	2	-3
SWP58213	43	42	1	-3	SWP58269	143	140	1	-2
SWP58218	12	10	1	-3	SWP58270	159	157	2	-3
SWP58219	21	19	2	-3	SWP58271	143	141	2	-4
SWP58220	28	26	1	-3	SWP58272	164	161	2	-3
SWP58221	30	27	1	-2	SWP58273	161	158	2	-3
SWP58222	45	43	2	-3	SWP58275	12	8	2	-2
SWP58223	53	50	1	-2	SWP58276	10	5	2	-2
SWP58224	80	77	1	-2	SWP58277	22	18	2	-3
SWP58225	69	66	1	-2	SWP58278	34	32	2	-3
SWP58226	71	69	2	-3	SWP58279	31	27	3	-4
SWP58227	91	89	1	-2	SWP58280	28	26	2	-3
SWP58228	95	94	1	-3	SWP58281	73	69	2	-3
SWP58229	132	130	1	-3	SWP58282	64	60	2	-3
SWP58230	96	93	1	-2	SWP58283	66	65	1	-2
SWP58231	138	137	1	-4	SWP58284	76	75	1	-3
SWP58233	12	10	2	-3	SWP58285	68	66	1	-3
SWP58235	25	22	2	-3	SWP58287	81	79	1	-3
SWP58236	23	21	2	-3	SWP58288	95	93	1	-3
SWP58237	33	30	2	-3	SWP58289	86	83	2	-3
SWP58238	31	28	2	-3	SWP58290	102	99	2	-4
SWP58239	38	34	1	-2	SWP58291	117	114	1	-2
SWP58240	55	53	2	-4	SWP58292	111	109	1	-3
SWP58241	70	68	2	-3	SWP58293	9	7	1	-3
SWP58242	105	102	2	-3	SWP58294	11	9	2	-4
SWP58243	119	117	2	-4	SWP58295	20	18	1	-3
SWP58244	130	128	1	-3	SWP58296	30	29	1	-3
SWP58245	102	100	1	-3	SWP58297	47	45	1	-3
SWP58246	98	96	1	-3	SWP58298	53	51	1	-3
SWP58247	90	89	1	-3	SWP58299	69	66	1	-2
SWP58248	116	113	1	-2	SWP58300	74	72	1	-3

Table 3 continued

Image	O_{159}	C_{159}	θ_u	θ_l	Image	O_{159}	C_{159}	θ_u	θ_l
SWP58301	84	82	1	-2	SWP58336	80	79	1	-3
SWP58302	98	96	2	-3	SWP58337	73	72	1	-3
SWP58303	106	103	2	-3	SWP58338	110	108	1	-2
SWP58304	108	106	1	-2	SWP58342	13	11	1	-2
SWP58305	164	161	2	-3	SWP58344	23	18	4	-5
SWP58306	166	164	2	-3	SWP58345	8	7	1	-2
SWP58307	150	147	1	-3	SWP58346	95	94	1	-3
SWP58308	143	141	1	-3	SWP58347	95	94	1	-3
SWP58311	14	11	2	-3	SWP58352	13	12	1	-2
SWP58312	23	20	2	-2	SWP58353	7	6	1	-2
SWP58313	21	19	2	-3	SWP58355	62	61	1	-2
SWP58314	27	24	2	-3	SWP58356	74	73	1	-3
SWP58315	37	34	2	-3	SWP58361	2655	923	252	-252
SWP58316	48	46	2	-3	SWP58362	29	28	1	-2
SWP58317	48	45	2	-3	SWP58363	72	71	1	-2
SWP58318	62	59	2	-3	SWP58364	91	90	1	-3
SWP58319	81	79	2	-4	SWP58365	87	85	1	-2
SWP58320	126	123	2	-3	SWP58369	6	5	1	-2
SWP58321	132	129	2	-3	SWP58371	6	5	1	-2
SWP58322	142	139	1	-2	SWP58374	18	15	1	-2
SWP58323	97	96	1	-2	SWP58375	29	27	1	-3
SWP58324	104	103	1	-3	SWP58376	40	37	1	-2
SWP58325	95	94	1	-3	SWP58377	38	35	1	-2
SWP58326	100	98	1	-2	SWP58378	44	42	1	-3
SWP58327	92	91	1	-3	SWP58379	39	37	2	-3
SWP58328	103	102	1	-3	SWP58380	48	45	1	-3
SWP58329	105	103	1	-2	SWP58381	55	52	1	-2
SWP58330	106	105	1	-3	SWP58382	67	65	2	-3
SWP58332	16	13	2	-3	SWP58383	17	16	1	-2
SWP58334	7	6	1	-2	SWP58384	457	448	4	-4
SWP58335	74	73	1	-3					

Table 4

Image	O_{159}	C_{159}	θ_u	θ_l	Image	O_{159}	C_{159}	θ_u	θ_l
LWP29320	112	86	29	-29	LWP30783	229	89	22	-22
LWP29347	421	163	59	-59	LWP30784	362	228	23	-23
LWP29535	30	28	1	-3	LWP30785	266	125	23	-23
LWP29536	14	12	2	-3	LWP30786	96	33	9	-9
LWP29586	108	41	14	-14	LWP31037	97	39	14	-14
LWP29620	9	6	1	-2	LWP31222	29	24	4	-5
LWP29664	213	163	48	-48	LWP31237	12	11	1	-3
LWP29687	143	72	11	-11	LWP31238	30	28	1	-3
LWP29691	39	16	5	-5	LWP31241	410	317	15	-15
LWP29832	14	12	1	-3	LWP31244	11	8	2	-3
LWP29833	92	38	11	-11	LWP31245	10	8	1	-2
LWP29834	154	92	10	-10	LWP31246	17	14	2	-3
LWP29837	80	77	1	-2	LWP31248	22	19	2	-3
LWP29884	492	373	83	-83	LWP31249	13	9	1	-2
LWP29966	11	7	2	-3	LWP31250	15	11	3	-4
LWP29988	9	6	2	-3	LWP31252	29	16	4	-4
LWP30012	101	97	4	-4	LWP31257	11	8	1	-2
LWP30050	9	4	1	-2	LWP31258	28	25	2	-3
LWP30081	9	5	2	-2	LWP31264	11	7	2	-3
LWP30155	76	33	9	-9	LWP31294	216	77	20	-20
LWP30170	107	46	15	-15	LWP31295	286	135	26	-26
LWP30196	125	46	13	-13	LWP31297	182	87	10	-10
LWP30251	108	51	17	-17	LWP31315	3415	815	306	-306
LWP30308	9	4	1	-2	LWP31316	4117	1142	375	-375
LWP30317	135	102	9	-9	LWP31317	4996	3083	296	-296
LWP30331	9	6	2	-3	LWP31319	1939	1534	92	-92
LWP30363	7	5	1	-2	LWP31320	3908	1174	407	-407
LWP30428	187	83	23	-23	LWP31321	3721	864	326	-326
LWP30430	241	91	23	-23	LWP31322	237	233	4	-4
LWP30431	195	77	18	-18	LWP31323	206	130	20	-20
LWP30494	10	7	2	-3	LWP31324	11320	10343	193	-193
LWP30507	13	11	1	-3	LWP31327	3794	1182	333	-333
LWP30532	9	4	2	-2	LWP31329	2081	1895	29	-29
LWP30550	7	5	1	-2	LWP31342	219	73	25	-25
LWP30565	9	7	1	-2	LWP31364	93	53	11	-11
LWP30638	182	85	26	-26	LWP31365	79	25	7	-7
LWP30648	13	10	1	-2	LWP31370	41	39	1	-2
LWP30649	14	11	2	-3	LWP31372	17	14	1	-2
LWP30664	7	5	1	-2	LWP31379	51	46	2	-3
LWP30688	210	86	28	-28	LWP31385	9	6	1	-2
LWP30782	153	58	18	-18	LWP31394	40	19	6	-6

Table 4 continued

Image	O_{159}	C_{159}	θ_u	θ_l	Image	O_{159}	C_{159}	θ_u	θ_l
LWP31397	14	11	2	-3	LWP31616	13	9	2	-3
LWP31400	107	29	9	-9	LWP31634	35	33	2	-3
LWP31403	14	12	1	-3	LWP31635	23	20	2	-3
LWP31404	9	7	1	-3	LWP31636	12	11	1	-2
LWP31412	30	20	5	-5	LWP31638	186	180	5	-6
LWP31420	24	15	4	-5	LWP31663	172	158	10	-10
LWP31422	87	32	8	-8	LWP31664	22	18	2	-2
LWP31426	81	48	9	-9	LWP31665	26	24	1	-2
LWP31427	68	40	11	-11	LWP31666	80	78	1	-2
LWP31428	219	157	11	-11	LWP31670	11	8	2	-3
LWP31429	415	371	11	-11	LWP31672	10	6	2	-2
LWP31430	387	329	8	-8	LWP31674	44	41	1	-3
LWP31431	147	118	7	-7	LWP31675	10	7	1	-2
LWP31432	110	70	16	-16	LWP31676	252	188	13	-13
LWP31433	103	61	16	-16	LWP31683	214	145	15	-15
LWP31434	79	32	10	-10	LWP31684	356	271	12	-12
LWP31437	84	48	8	-8	LWP31685	394	310	8	-8
LWP31438	201	154	12	-12	LWP31686	1006	871	18	-18
LWP31439	470	415	8	-8	LWP31687	990	843	12	-12
LWP31440	213	160	10	-10	LWP31703	242	73	23	-23
LWP31444	30	27	3	-4	LWP31705	320	167	15	-15
LWP31447	170	75	12	-12	LWP31706	317	113	31	-31
LWP31451	141	59	16	-16	LWP31707	119	34	11	-11
LWP31456	25	15	4	-5	LWP31708	283	149	18	-18
LWP31458	32	26	3	-4	LWP31709	373	140	20	-20
LWP31460	39	25	6	-6	LWP31716	180	89	12	-12
LWP31461	9	5	1	-2	LWP31717	467	264	28	-28
LWP31482	281	186	16	-16	LWP31718	402	275	20	-20
LWP31485	8	5	1	-2	LWP31721	468	377	18	-18
LWP31486	51	42	3	-3	LWP31722	766	705	10	-10
LWP31487	277	227	8	-8	LWP31723	1627	1476	20	-20
LWP31507	13	11	2	-3	LWP31724	1034	864	25	-25
LWP31509	274	200	16	-16	LWP31725	29	20	4	-4
LWP31516	262	203	17	-17	LWP31726	16	14	1	-2
LWP31517	159	100	9	-9	LWP31739	66	53	6	-6
LWP31522	17	15	2	-3	LWP31740	652	496	28	-28
LWP31534	322	241	10	-10	LWP31744	110	107	2	-3
LWP31536	6	5	1	-2	LWP31749	262	244	9	-9
LWP31547	24	20	6	-6	LWP31755	382	306	16	-16
LWP31567	26	20	4	-5	LWP31758	9	6	1	-2
LWP31572	155	54	16	-16	LWP31759	15	13	1	-3

Table 4 continued

Image	O_{159}	C_{159}	θ_u	θ_l	Image	O_{159}	C_{159}	θ_u	θ_l
LWP31760	45	41	1	-2	LWP31976	182	79	12	-12
LWP31763	1709	1608	17	-17	LWP31977	19	12	3	-4
LWP31764	483	365	17	-17	LWP31978	7	5	1	-2
LWP31765	3237	3106	19	-19	LWP31983	231	141	14	-14
LWP31766	34	32	1	-2	LWP31991	332	172	19	-19
LWP31767	22	20	1	-2	LWP31994	1119	970	21	-21
LWP31772	543	480	13	-13	LWP31996	235	88	24	-24
LWP31773	29	27	1	-2	LWP31998	219	49	17	-17
LWP31778	256	253	2	-3	LWP32000	1500	1377	18	-18
LWP31786	444	368	88	-88	LWP32003	228	160	19	-19
LWP31787	5562	2189	440	-440	LWP32004	394	300	12	-12
LWP31788	4780	1400	443	-443	LWP32005	363	277	14	-14
LWP31789	5146	1739	439	-439	LWP32006	451	370	13	-13
LWP31790	5405	1863	418	-418	LWP32011	33	23	3	-4
LWP31807	17	7	2	-3	LWP32012	8	7	1	-2
LWP31812	18	14	2	-3	LWP32013	7	6	1	-1
LWP31824	30	27	2	-3	LWP32027	123	51	13	-13
LWP31834	274	125	23	-23	LWP32028	186	100	13	-13
LWP31835	271	209	14	-14	LWP32029	146	95	9	-9
LWP31838	378	283	17	-17	LWP32036	14	10	2	-3
LWP31839	14	11	1	-2	LWP32042	9	8	1	-2
LWP31841	48	23	5	-5	LWP32044	10	8	1	-2
LWP31853	10	6	1	-2	LWP32046	18	17	1	-2
LWP31856	770	492	31	-31	LWP32047	218	212	3	-3
LWP31880	134	57	13	-13	LWP32049	16	13	2	-2
LWP31902	21	16	3	-4	LWP32050	111	85	7	-7
LWP31909	10	6	2	-2	LWP32051	26	24	1	-3
LWP31910	21	18	1	-2	LWP32052	496	447	8	-8
LWP31918	6	5	1	-1	LWP32058	12	7	2	-2
LWP31921	217	129	15	-15	LWP32060	28	26	1	-3
LWP31924	154	148	3	-4	LWP32062	94	57	12	-12
LWP31926	11	9	2	-3	LWP32071	8626	8450	35	-35
LWP31931	218	67	20	-20	LWP32072	97872	93836	250	-250
LWP31933	1069	952	26	-26	LWP32074	3682	3745	85	-85
LWP31934	615	537	14	-14	LWP32075	85992	81899	245	-245
LWP31951	818	711	18	-18	LWP32076	60892	59822	42	-42
LWP31953	1037	976	16	-16	LWP32078	4121	4070	11	-11
LWP31958	15	14	1	-2	LWP32079	10992	10827	33	-33
LWP31967	17	14	2	-3	LWP32081	75	73	1	-3
LWP31973	356	273	14	-14	LWP32082	30	29	1	-3
LWP31975	204	106	13	-13	LWP32086	14	12	1	-2

Table 4 continued

Image	O_{159}	C_{159}	θ_u	θ_l	Image	O_{159}	C_{159}	θ_u	θ_l
LWP32088	31	20	4	-4	LWP32254	14	13	1	-3
LWP32089	25	22	2	-3	LWP32255	8	6	1	-2
LWP32096	45	42	2	-3	LWP32256	294	285	3	-4
LWP32102	8	6	1	-3	LWP32269	95	87	3	-4
LWP32104	12	7	2	-2	LWP32288	11	7	2	-3
LWP32107	9	6	2	-3	LWP32289	60	58	2	-3
LWP32108	26	23	1	-2	LWP32299	6	5	1	-2
LWP32113	139	88	13	-13	LWP32301	388	323	15	-15
LWP32115	239	176	12	-12	LWP32304	17	14	1	-2
LWP32118	540	504	16	-16	LWP32305	9	8	1	-3
LWP32121	317	248	10	-10	LWP32307	33	31	1	-2
LWP32126	139	76	13	-13	LWP32309	431	356	11	-11
LWP32128	244	174	12	-12	LWP32312	749	682	13	-13
LWP32146	25	23	2	-4	LWP32313	433	353	10	-10
LWP32147	19	17	2	-4	LWP32319	1335	1288	13	-13
LWP32148	8155	7011	119	-119	LWP32322	1122	1051	11	-11
LWP32152	1592	1344	25	-25	LWP32323	965	913	11	-11
LWP32153	50	45	4	-5	LWP32330	106	100	3	-4
LWP32155	19	17	2	-3	LWP32340	45	25	8	-8
LWP32158	12760	10544	191	-191	LWP32341	321	73	28	-28
LWP32159	27397	25117	176	-176	LWP32353	9	8	1	-3
LWP32168	854	763	15	-15	LWP32354	12	10	2	-4
LWP32169	3320	1447	179	-179	LWP32357	29	26	2	-3
LWP32170	4819	3514	108	-108	LWP32358	22	19	2	-2
LWP32184	13	11	1	-2	LWP32359	26	22	2	-3
LWP32192	6	4	1	-2	LWP32361	3725	1682	187	-187
LWP32193	8	7	1	-2	LWP32366	424	354	12	-12
LWP32199	29	25	3	-4	LWP32367	300	227	12	-12
LWP32200	36	29	2	-3	LWP32368	175	153	12	-12
LWP32203	116	111	2	-3	LWP32395	24	20	2	-3
LWP32204	6	4	1	-2	LWP32396	39	35	2	-3
LWP32205	143	139	2	-3	LWP32397	51	48	2	-3
LWP32208	155	150	2	-3	LWP32398	65	61	2	-3
LWP32210	13	8	2	-3	LWP32399	44	42	2	-3
LWP32211	20	13	3	-3	LWP32400	33	30	3	-4
LWP32219	8	7	1	-2	LWP32401	86	82	3	-4
LWP32229	104	100	3	-4	LWP32402	88	84	1	-2
LWP32241	15	12	2	-4	LWP32403	49	46	2	-3
LWP32243	11	9	1	-3	LWP32404	54	51	2	-3
LWP32251	28	22	2	-3	LWP32405	91	89	2	-3
LWP32253	23	21	1	-3	LWP32406	55	51	2	-2

Table 4 continued

Image	O_{159}	C_{159}	θ_u	θ_l	Image	O_{159}	C_{159}	θ_u	θ_l
LWP32407	35	31	2	-3	LWP32450	114	112	1	-3
LWP32408	40	37	2	-3	LWP32451	105	102	2	-3
LWP32409	141	139	1	-3	LWP32452	112	109	2	-3
LWP32410	123	121	2	-3	LWP32453	105	103	2	-3
LWP32411	118	115	1	-2	LWP32454	160	155	4	-5
LWP32412	130	128	2	-4	LWP32455	60	58	1	-3
LWP32413	94	92	1	-3	LWP32456	43	40	2	-4
LWP32414	113	111	1	-3	LWP32457	101	98	2	-3
LWP32415	100	99	1	-3	LWP32458	90	89	1	-3
LWP32416	116	114	2	-3	LWP32459	121	119	2	-3
LWP32417	128	125	1	-2	LWP32460	131	129	2	-4
LWP32418	108	106	1	-3	LWP32461	99	97	1	-3
LWP32419	52	51	1	-3	LWP32462	135	132	1	-2
LWP32420	62	60	1	-3	LWP32463	127	124	2	-4
LWP32421	80	78	2	-3	LWP32464	99	96	1	-2
LWP32422	83	81	2	-3	LWP32465	122	120	2	-3
LWP32423	62	59	2	-3	LWP32466	128	125	2	-4
LWP32424	16	15	1	-2	LWP32467	116	112	2	-4
LWP32426	105	100	2	-3	LWP32468	156	152	3	-4
LWP32427	125	120	2	-3	LWP32469	47	46	1	-3
LWP32428	117	110	2	-4	LWP32470	66	64	1	-3
LWP32429	140	135	2	-3	LWP32471	134	132	2	-3
LWP32430	137	132	2	-4	LWP32472	137	135	2	-3
LWP32431	96	94	1	-2	LWP32473	127	125	1	-3
LWP32432	125	123	1	-2	LWP32474	141	138	2	-4
LWP32433	111	109	1	-3	LWP32475	129	127	2	-4
LWP32434	114	111	2	-4	LWP32476	133	131	2	-3
LWP32435	129	126	1	-3	LWP32477	129	127	2	-4
LWP32436	101	99	1	-3	LWP32478	142	140	2	-4
LWP32437	119	117	1	-3	LWP32479	126	124	2	-3
LWP32438	85	82	1	-3	LWP32480	146	142	2	-4
LWP32439	47	45	1	-2	LWP32481	143	138	4	-5
LWP32441	66	64	2	-3	LWP32482	77	75	2	-3
LWP32442	51	50	1	-3	LWP32483	110	108	1	-3
LWP32443	100	98	1	-2	LWP32484	121	119	2	-5
LWP32444	95	92	1	-2	LWP32485	148	145	1	-2
LWP32445	51	49	1	-2	LWP32486	133	132	1	-3
LWP32446	101	100	1	-3	LWP32487	129	127	2	-4
LWP32447	133	131	1	-3	LWP32488	149	147	1	-3
LWP32448	145	143	1	-3	LWP32489	124	122	2	-3
LWP32449	123	121	2	-3	LWP32490	122	119	2	-3

Table 4 continued

Image	O_{159}	C_{159}	θ_u	θ_l	Image	O_{159}	C_{159}	θ_u	θ_l
LWP32491	143	141	1	-3	LWP32561	38	35	2	-3
LWP32492	128	126	1	-3	LWP32568	45	27	8	-8
LWP32493	90	88	2	-4	LWP32575	1066	522	161	-161
LWP32494	37	34	2	-3	LWP32576	601	289	82	-82
LWP32495	52	50	1	-3	LWP32580	1073	765	46	-46
LWP32496	93	91	2	-3	LWP32585	20	18	1	-3
LWP32497	125	122	2	-4	LWP32586	13	11	1	-2
LWP32498	132	129	2	-4	LWP32587	34	32	1	-2
LWP32499	129	127	1	-3	LWP32588	22	19	2	-3
LWP32500	151	149	1	-2	LWP32589	22	20	2	-3
LWP32501	6	5	1	-2	LWP32590	52	50	1	-2
LWP32510	8	7	1	-2	LWP32591	47	46	1	-3
LWP32511	42	41	1	-2	LWP32592	59	57	1	-3
LWP32512	368	364	3	-4	LWP32593	60	58	1	-2
LWP32513	142	141	1	-3	LWP32594	50	48	1	-3
LWP32514	11	10	1	-2	LWP32597	7	6	1	-2
LWP32515	151	149	1	-3	LWP32599	15	13	1	-2
LWP32516	172	171	1	-3	LWP32600	21	18	2	-3
LWP32517	155	153	1	-3	LWP32601	43	39	2	-3
LWP32518	171	169	1	-2	LWP32603	16	14	1	-1
LWP32519	146	145	1	-3	LWP32604	61	59	2	-3
LWP32520	166	165	1	-3	LWP32605	84	82	1	-3
LWP32521	189	187	1	-3	LWP32606	18	16	2	-4
LWP32522	191	176	6	-6	LWP32607	9	5	2	-2
LWP32524	444	425	10	-10	LWP32608	14	12	1	-3
LWP32526	467	450	14	-14	LWP32609	33	29	1	-2
LWP32528	1196	1172	15	-15	LWP32610	14	12	1	-3
LWP32530	2350	2327	18	-18	LWP32612	37	35	2	-3
LWP32532	2514	2474	13	-13	LWP32614	12	10	1	-3
LWP32534	2357	2310	12	-12	LWP32615	24	21	2	-3
LWP32535	104	101	2	-3	LWP32616	31	29	2	-3
LWP32537	134	131	2	-3	LWP32617	43	41	1	-3
LWP32539	119	116	2	-3	LWP32618	59	58	1	-3
LWP32541	170	168	1	-2	LWP32619	61	58	1	-3
LWP32543	170	169	1	-3	LWP32620	74	71	1	-3
LWP32544	157	153	3	-4	LWP32621	18	16	2	-4
LWP32552	13	12	1	-3	LWP32622	21	19	2	-3
LWP32554	29	25	1	-2	LWP32623	40	38	1	-3
LWP32555	323	314	3	-3	LWP32624	29	28	1	-3
LWP32559	15	13	1	-2	LWP32625	22	21	1	-2
LWP32560	220	170	12	-12	LWP32626	49	46	1	-2

Table 4 continued

Image	O_{159}	C_{159}	θ_u	θ_l	Image	O_{159}	C_{159}	θ_u	θ_l
LWP32627	84	82	1	-2	LWP32663	119	116	1	-2
LWP32628	28	27	1	-2	LWP32667	30	27	2	-3
LWP32629	38	36	1	-2	LWP32669	68	65	1	-2
LWP32630	107	106	1	-3	LWP32670	16	15	1	-2
LWP32631	122	121	1	-3	LWP32671	114	111	2	-3
LWP32632	29	26	1	-2	LWP32672	133	131	2	-4
LWP32633	31	28	1	-2	LWP32673	268	262	4	-5
LWP32634	36	34	1	-3	LWP32675	107	105	1	-3
LWP32635	8	6	1	-2	LWP32676	12	11	1	-1
LWP32636	19	17	1	-2	LWP32677	133	132	1	-3
LWP32637	42	39	1	-2	LWP32681	11	8	2	-3
LWP32638	80	78	2	-3	LWP32682	67	60	3	-4
LWP32639	18	17	1	-2	LWP32683	48	44	2	-2
LWP32640	28	26	1	-2	LWP32684	156	149	2	-3
LWP32641	91	89	1	-2	LWP32685	7	6	1	-2
LWP32642	107	105	1	-3	LWP32686	93	90	1	-2
LWP32646	50	47	2	-4	LWP32687	16	15	1	-2
LWP32647	71	68	2	-3	LWP32688	113	110	2	-4
LWP32648	104	103	1	-3	LWP32689	12	11	1	-2
LWP32651	144	142	1	-2	LWP32690	156	155	1	-3
LWP32653	113	112	1	-3	LWP32691	140	139	1	-3
LWP32654	10	6	2	-2	LWP32693	15	14	1	-2
LWP32656	74	70	2	-4	LWP32694	305	300	3	-3